東海大学海洋研究所報告書　第 35 号(2014) 43～ 52 頁　原著論文(Original Article)
Bull Inst. Oceanic Res. & Develop. Tokai Univ. (2014), 43, 1-52

Preliminary Analyses of Micro Pressure Data Associated with Volcanic Eruption near Nishinoshima, Tsunami, and Storm at Ogasawara, Japan

Fei Zhang [1), 2), 3)], Maho Nakamura [1)], Yuko Suzuki [1)], Yoshiaki Orihara [1), 4)], Chiaki Tsurudome [1)], Daiki Ikeda [1)], Kosei Ohora [1)], Jann-Yenq Liu [1), 2), 3)], Masashi Kamogawa [1), *)]

Abstract

We report data quality of a micro barometer which observes atmospheric infrasonic waves at Ogasawara islands, approximately 1000 kilometers south of Tokyo, Japan, showing the cases of three different natural events including volcanic eruption, tsunami, strong wind and signals from one ordinary day. With considering weather conditions, the wavelet spectrum analysis showed different features. The good quality of Ogasawara data is verified, partly because microbarom caused by the nonlinear interaction of large-amplitude storm-generated waves on the surface of the ocean has been clearly observed.

1. Introduction

Inaudible infrasound propagates thousands of kilometers through ducts formed in the troposphere, stratosphere, and lower thermosphere. While there are several modes for propagation, dominant one ducts between the earth's surface and a stratospheric region at a height of about 50 kilometers. There are many natural sources of infrasound such as meteors, volcanic eruptions, ocean waves, avalanches, tsunamis, wind and any event which lead to slow oscillations of the air. Man-made sources are explosions, large combustion processes, slow speed fans and machinery, etc.

Microbarometers, one of sensitive barometers, that measure air pressure with high precision, have been used to monitor compliance with the Comprehensive Nuclear-Test-Ban Treaty by detecting the infrasound signature of a nuclear explosion (see Alcoverro et al., 2005; Alcoverro, 2008; Zumberge

1) Department of Physics, Tokyo Gakugei University, 4-1-1 Nukuikitamachi, Koganeishi, Tokyo 184-8501, Japan.
2) Institute of Space Science, National Central University, No.300 Jhongda Road, Jhongli City, Taoyuan County 32001, Taiwan.
3) College of Mechanical Engineering and Applied Electronics Technology, Beijing University of Technology, No. 100 Pingleyuan, Chaoyang District, Beijing 100124, China.
4) Institute of Oceanic Research and Development, Tokai University, 3-20-1 Orido, Shimizu-ku, Shizuoka 424-8610, Japan.
*) Corresponding author
(2014 年 2 月 17 日受付／2014 年 3 月 24 日受理)

et al., 2003; Catherine *et al.*, 2013). Numerous volcanic eruptions and explosions have been detected by infrasound measurement during the last decades (see, e.g., Goerke *et al.*, 1965; Le Pichon *et al.*, 2005; Liszka and Garcés, 2002). The dominant frequency and amplitude of infrasonic waves from volcanic explosions depends on the size of the explosion and the distance from the source. In addition, severe convective storms and meteorological sources like tornadoes, lightning and sprites also generate infrasound with frequencies between 0.02 and 0.1 Hz. The source mechanism for these waves is better understood now (Farges and Blanc, 2010; Liszka and Hobara, 2006; Assink *et al.*, 2008). Arai *et al.* (2011) investigated atmospheric pressure changes caused by the 2011 Off the Pacific Coast of Tohoku earthquake (Mw9.0) recorded by sensitive microbarographs. They verified that the co-seismic atmospheric boundary waves were excited by the uplift and subsidence of the ocean surface.

Japan has several arcs generating various tectonic activities including volcanic eruptions and large earthquakes. In order to better understand these events, a microbarometer was installed by Tokyo Gakugei University (TGU) in June, 2013 at Ogasawara islands, 1000 kilometers south of Tokyo, Japan. Several interesting events have been recorded by this micro barometer during last 6 months. Taking into account meteorological conditions, four typical events were analyzed with wavelet analysis to evaluate the quality of data at Ogasawara.

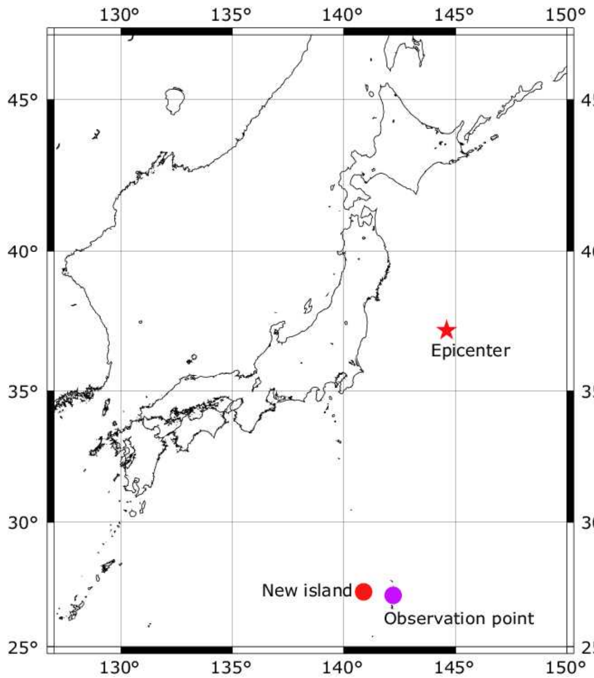

Fig. 1 Location of our micro barometer. Red star denotes the epicenter of one M7.1 earthquake at 1710 UT on 25 October, 2013; Red and purple circles denote the new island and our observation point, respectively.

2. Observation and Methodology

Quartz-pressure-transducer-type microbarometer (Toho Mercantile, Co. Ltd.) capable of recording the absolute atmospheric pressure with a resolution of 0.001 hPa at 2 Hz sampling rate was installed in Ogasawara, Japan as shown in Fig. 1 and recorded pressure during last 6 months. Fig. 2 shows an example of the time series of pressures recorded by ours (Tokyo Gakugei University) and Japan Meteorological Agency (JMA) at Ogasawara at the same period (From 1500 UT on 25 October, 2013 to 1500 UT on 26 October, 2013) (http://www.jma.go.jp/jma/index.html). Note that resolution and sampling rate of the microbarometer installed by JMA are 0.3 hPa and 0.002 Hz, respectively. Two time series are shown so that a good correlation is found as shown in Fig. 3. Almost all the points are located on the diagonal line. Statistical analysis demonstrated that correlation coefficients of 99% of the data are larger t.han 0.99

Compared with the common FFT method, wavelet is more suitable for continuous and unstable signals. In this paper, we use wavelet method to analyze the raw data of pressure. We also adopt multiband narrow filter method to roughly observe the frequency contents.

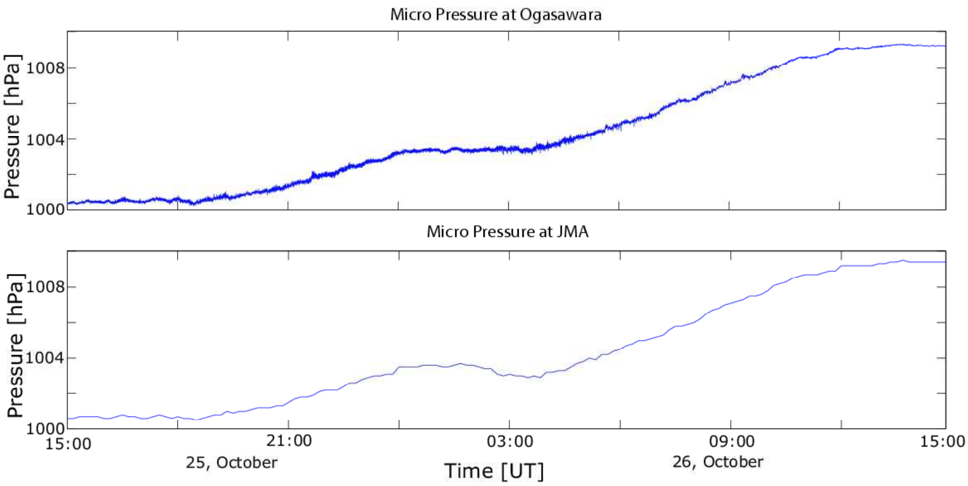

Fig. 2 Infrasound signals from 1500 UT on 25 October, 2013 to 1500 UT on 26 October, 2013. A top and bottom panels are raw data of pressure recorded by ours and JMA at Ogasawara, respectively.

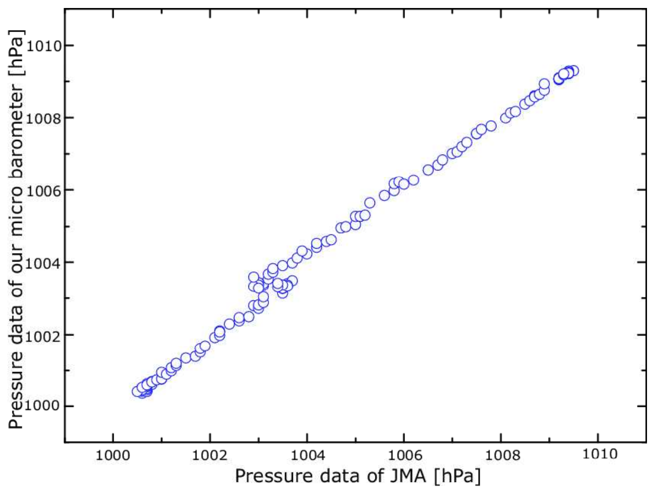

Fig. 3 Correlation of micro pressure data recorded by ours and JMA at Ogasawara.

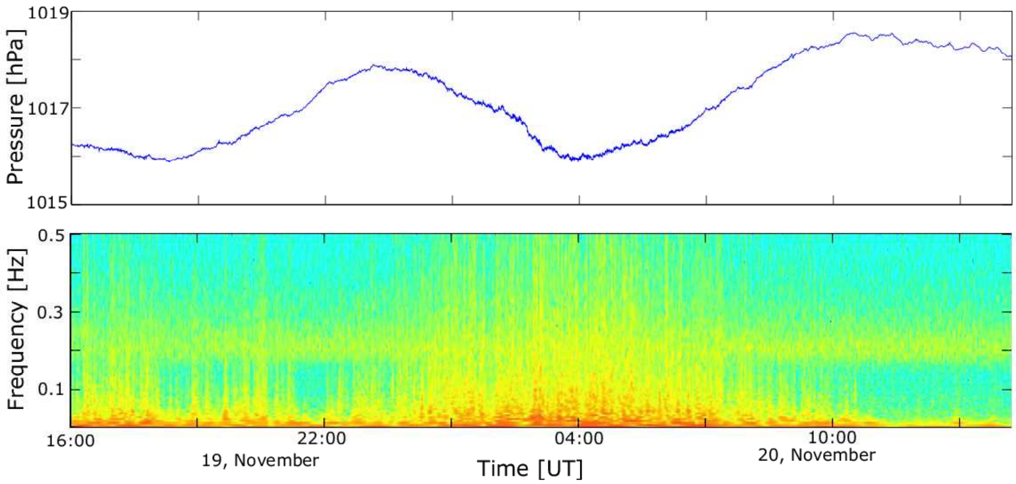

Fig. 4 Infrasound signals possibly from a small volcanic event. The top panel is raw data and the bottom panel is wavelet spectrum data.

3. Results

3.1 Volcanic Eruption

A volcanic eruption occurred near Nishinoshima Island, which locates 130 km west of Chichi–jima in Ogasawara islands. Since there is no scientific observation around the new island, we knew that the volcanic eruption was confirmed on 20 November, 2013 by means of aerial survey. Figure 4 is expected to present volcanic events recorded by our micro barometer located 120 kilometers away from the new island. A top panel of Fig. 4 shows the raw data of this event and fluctuations from 0100UT to 0700UT were found. A next panel shows a spectrum by means of wavelet method. This panel shows a broadband infrasound accompanying high frequency component. Since similar cases, the eruption of Tungurahua Volcano, Ecuador, in August 2006 (Fee *et al.,* 2010) was recognized. We inferred that the eruption begin gradually around 2200 UT on 19 November and ended with evident shift to lower frequencies on 20, November.

In the lower panel of Fig. 4, continuous variations between 0.15 and 0.25 Hz were found. This is an intensive continuous infrasound waves propagating over a large distance due to the interaction of ocean swell with the atmosphere which is termed microbarom. We compare meteorological wind speed with the observed pressure. Fig. 5(a) shows the mean and the maximum wind speed for a sampling of 10 minutes drawn in red and blue lines, respectively. We found a small increase of wind speed and a broad spectrum of pressure shown in the lower panel of Fig. 4 from 0100UT to 0700UT. There are two possibilities to explain the variations of pressure from 0100UT to 0700UT. On one hand, the broad spectrum may be caused by the sudden wind speed change. On the other hand, this is caused by the volcanic eruption. Since we cannot make sure the accurate volcanic eruption time, it is difficult for us to distinguish whether there are volcanic eruption signals inside if there is only one station.

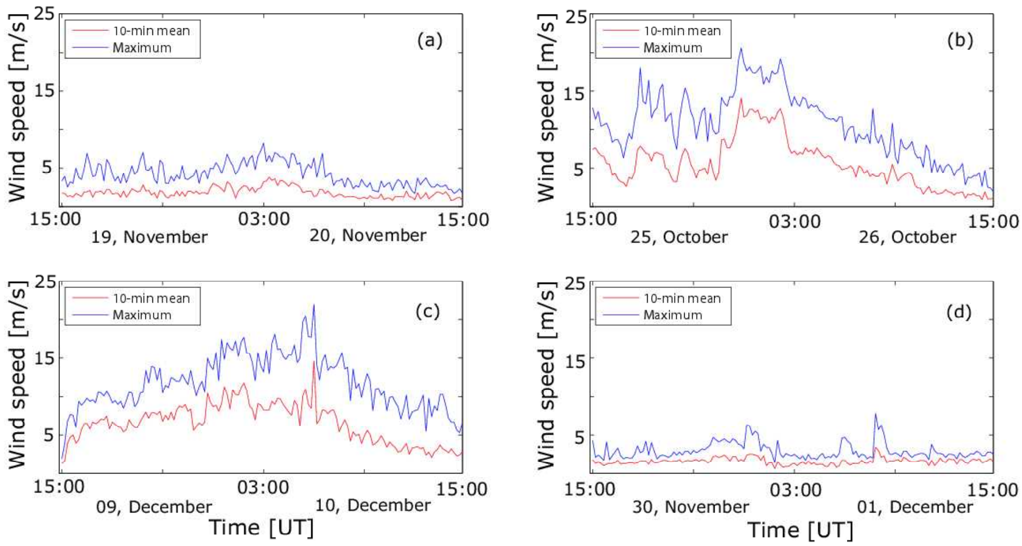

Fig. 5 Wind speed for four cases:
(a) Left and upper one: volcanic event on 20 November, 2013.
(b) Right and upper one: tsunami event on 25 October, 2013.
(c) Left and lower one: strong wind and rain event on 10 December, 2013.
(d) Right and lower one: ordinary signal event on 1 December, 2013.

3.2 Tsunami

Tsunami is one of infrasound sources (Le Pichon *et al*., 2005). An earthquake with a magnitude of 7.1 struck off the coast of Fukushima at 1710 UT on 25 October, 2013 (Fig. 1). The earthquake occurred 320 kilometers off the coast. About 40 minutes later, tsunami measuring up to 0.4 meters hit the coasts of Fukushima, Miyagi and Iwate, according to JMA (http://www.jma.go.jp/en/tsunami/focus_03_20131026025051.html). A top panel of Fig. 6 presents raw data from 0000UT of 25 October to 1400UT of 27 October, 2013. A huge pressure decreased by 21.51 hPa from standard atmospheric pressure. However, from the lower multiband filter panels, any useful information was not obtained. Ray tracing curves based on MSIS-E-90 Atmosphere Model (http://omniweb.gsfc.nasa.gov/vitmo/msis_vitmo.html) are shown in Fig. 7, following the calculation of Heki and Ping (2005). Estimated arrival time of infrasound at Ogasawara was 1748UT. Note that the distance between source and our micro barometer is about 1142 km.

According to Fig. 7, the propagation path from the Tsunami source area to the observation point also exists in the ionosphere. In order to verify that the sufficient intensity of tsunami-origin acoustic wave was not excited, the measurement of Global Positioning System total electron content (GPS TEC) (see Kakinami *et al*., 2012) is used. From GPS TEC measurement, the ionospheric disturbance generated by the tsunami-origin acoustic waves is confirmed. In this analysis, the F region is assumed to be a thin-layer located at 300 km altitude. The point of intersection between the ionospheric thin layer and the propagation path between the GPS

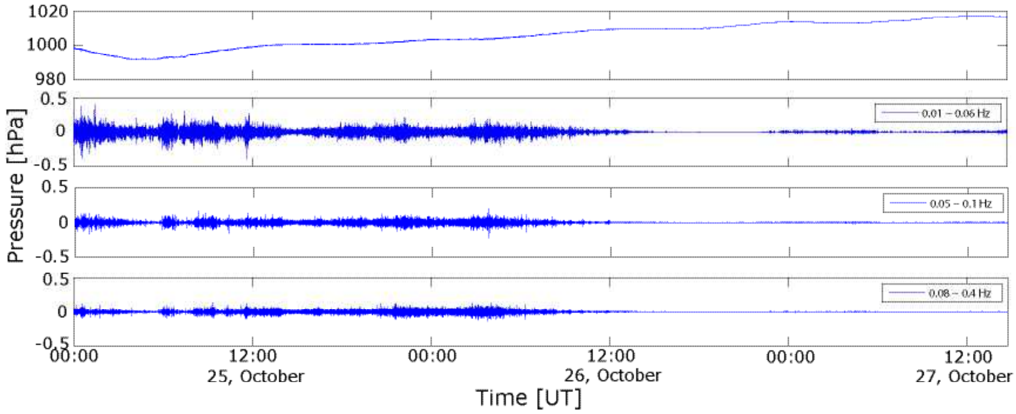

Fig. 6 A period of infrasound signals associated with a small tsunami on 25 October, 2013. Data are filtered between 0.01 and 0.4 Hz.

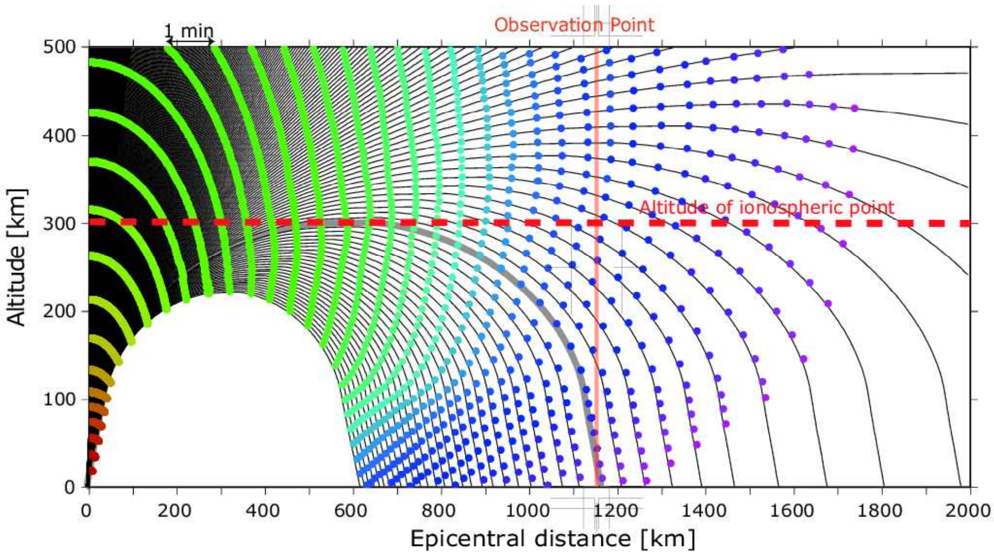

Fig. 7 Ray tracing curves on 25 October, 2013 based on MSIS-E-90 Atmosphere Model

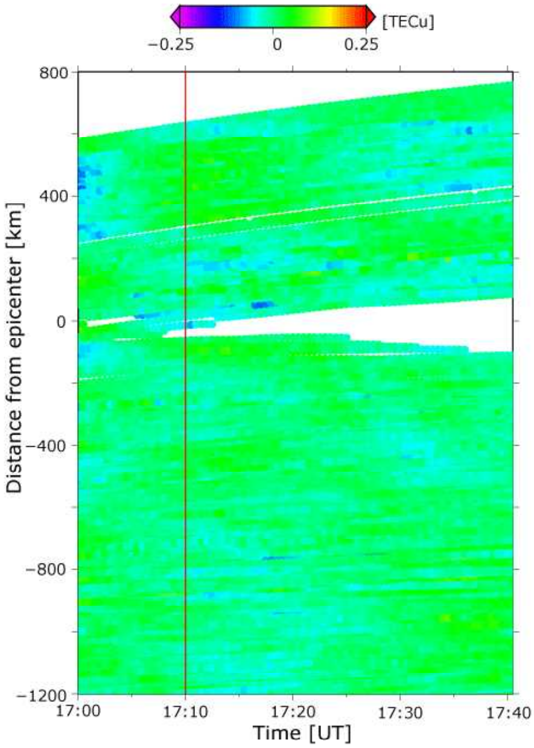

Fig. 8 Time series of TEC variation before and after tsunami on 25 October, 2013

satellites and their receivers is termed ionospheric point and its foot print on the ground surface is termed sub-ionospheric point (SIP). A sampling period of GEONET data is 30 seconds. In order to extract the TEC variation with a few minutes, we calculated the difference between the slant TEC and the least mean square estimation for 40 minutes before and 20 minutes after the mainshock and convert these difference into the vertical TEC (ΔvTEC) from the zenith angle of the GPS satellite direction. In Fig. 8, the time-series of ΔvTEC are drawn as the distance between the epicenter and the sub-ionospheric point. In this analysis, we have no signature of seismogenic ionospheric disturbance, as well as seismogenic infrasound from our pressure data.

In Fig. 9, wavelet method was used to reanalysis the period from 1600 UT of 25 October 2013 to 1400 UT of 25 October 2013. The major frequency of infrasound originating from tsunami ranges from 0.5 to 2 Hz (Le Pichon *et al*., 2005). from tsunami ranges from 0.5 to 2 Hz (Le Pichon *et al*., 2005). Fig. 9 shows large intensity from 0 to 0.3 Hz. Wind

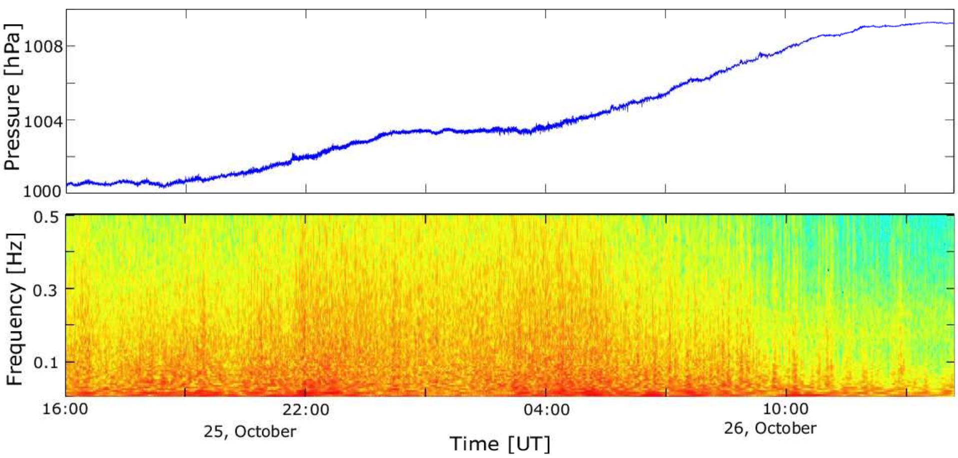

Fig. 9 Infrasound signals from a tsunami event caused by one earthquake.
The top panel is raw data and the bottom panel is wavelet spectrum data.

speed is larger than other day during our observation period as shown in Fig. 5(b). In general, wind-generated noise is the most major source of infrasonic background. In other words, strong wind hides weak signals. Therefore, even if we have an array observation of infrasound including more than three instruments and intensive signals generated by tsunami was emitted, it is difficult to discriminate the signals from the current observed data.

3.3 Strong Wind and Rain

One of infrasound sources with frequencies between 0.02 and 0.1 Hz is generated by severe convective storms. Other meteorological sources of infrasound such as microbursts, tornadoes, lightning and sprites have been also reported. Micro pressure variations associated with a thunderstorm is shown in Fig. 10. According to the meteorological conditions provided by JMA, strong wind due to severe storm occurred on 10 December, 2013 as shown in Fig. 5 (c). The dominant frequency is about 0.1 Hz when the pressure reaches the lowest. Furthermore, infrasonic waves caused by a lightning discharge during the storm also generate a clear sudden increase observed from three different frequency bands (Farges and Blanc, 2010). We found the lightning activities from 0300UT to 0500UT from our measurement of atmospheric electric field near the infrasound observation. Therefore, the signature shown in Fig. 11 is caused by lightning-related storm.

3.4 Ordinary Infrasound Signals

Micro barometer records many background noises at most time. The primary sources of background noise are given as follows: (1) Wind-generated micropressure fluctuations associated with turbulent eddies in the atmospheric boundary layer, of which intensity enhances in all frequencies. (2) Microbarom infrasonic waves in the 0.12–0.35 Hz passbands. The microbarom is almost always present at any point on the surface of the provided by JMA, strong wind due to severe storm occurred on 10 December, 2013 as shown in Fig. 5 (c). The dominant frequency is about 0.1 Hz when

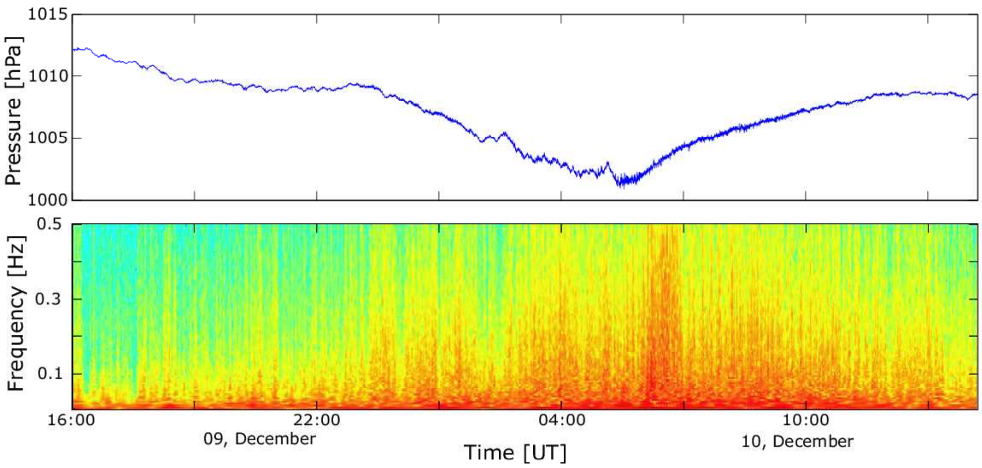

Fig. 10 Infrasound signals from a strong wind and rain event.
The top panel is raw data and the bottom panel is wavelet spectrum data.

the pressure reaches the lowest. Furthermore, infrasonic waves caused by a lightning discharge during the storm also generate a clear sudden increase observed from three different frequency bands (Farges and Blanc, 2010). We found the lightning activities from 0300UT to 0500UT from our measurement of atmospheric electric field near the infrasound observation. Therefore, the signature shown in Fig. 11 is caused by lightning-related storm.

3.4 Ordinary Infrasound Signals

Micro barometer records many background noises at most time. The primary sources of background noise are given as follows: (1) Wind-generated micropressure fluctuations associated with turbulent eddies in the atmospheric boundary layer, of which intensity enhances in all frequencies. (2) Microbarom infrasonic waves in the 0.12–0.35 Hz passbands. The microbarom is almost

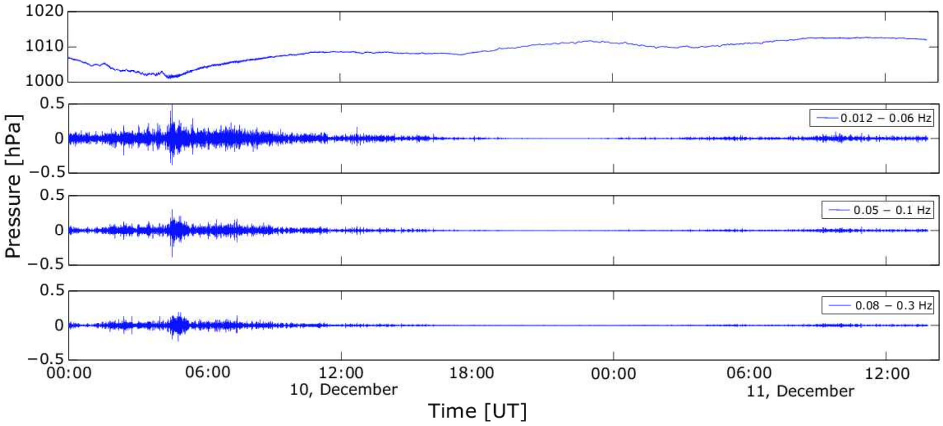

Fig. 11 A period of infrasound signals associated with a strong wind and rain on 10 December, 2013. Data are filtered between 0.012 and 0.3 Hz.

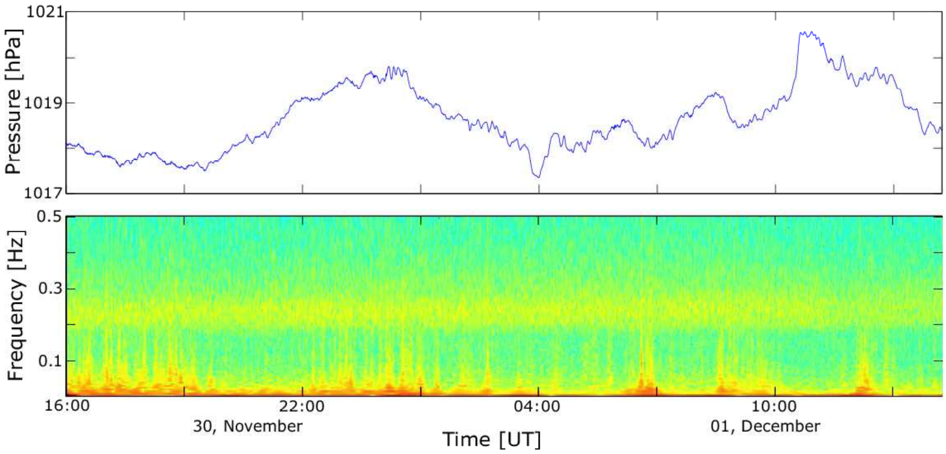

Fig. 12 Infrasound signals from ordinary event. The top panel is raw data and the bottom panel is wavelet spectrum data.

always present at any point on the surface of the globe at any time. We show the typical signals recorded under the circumstance without strong wind and rain,i. e. fair weather, as shown in Fig. 5 (d) on 1 December, 2013 in Fig. 12. Clear microbarom during the whole period was observed. How to reduce these mirccobarom is an important issue for infrasound research.

4. Conclusions

We report the preliminary results of infrasound recorded at Ogasawara islands, showing four typical cases to verify the data quality. Although significant events as volcano, tsunami, and storm could cause significant change, we partly show the signals related to them. In addition, we confirm the existence of microbarom in our observation points, so that we verify the sensitivity of our micro barometer.

Acknowledgements

We also thank S. Saito, S. Togo, Y. Suto, T. Shoji and R. Tanaka (Tokyo Gakugei University) for their supports for this analysis and T. Ohi (Toho Mercantile Co., Ltd.) for system installation. GPS and meteorological data in this study were provided by the Geographical Survey Institute of Japan and Japan Meteorological Agency. This research was supported by the Ministry of Education, Science, Sports and Culture, Scientific Research (B), No. 24310129, 2012 (M. K.).

References

Alcoverro, B., Martysevich, P., Starovoit, Y. (2005): Mechanical sensitivity of microbarometers MB2000 (DASE, France) and Chaparral 5 (USA) to vertical and horizontal ground motion. Inframatics, 9, 1–10.

Alcoverro, B. (2008): The design and performance of infrasound noise-reducing pipe arrays. Handbook of signal processing in acoustics, chap. 80, Springer, New York, 1473–1486.

Arai, N., Iwakuni, M., Watada, S., Imanishi, Y., Murayama, T., and Nogami, M. (2011): Atmospheric boundary waves excited by the tsunami generation related to the 2011 great Tohoku - Oki earthquake. Geophys. Res. Lett., 38, L00G18, doi:10.1029/2011GL049146.

Assink, J. D., Evers, L. G., Holleman, I., and Paulssen, H. (2008): Characterization of infrasound from lightning. Geophys Res Lett., 35, L15802.

Catherine, D. G. H, Michael, A. H. H., Kristoffer T. W. (2013): Detection of gravity waves across the US Array: A case study. Earth and Planetary Science Letters, http://dx.doi.org/10.1016/j.epsl.2013.06.042.

Farges, T., and Blanc, E., (2010): Characteristics of infrasound from lightning and sprites near thunderstorm areas. J. Geophys. Res., 115, A00E31, doi:10.1029/2009JA014700.

Fee, D., Garces, M., and Steffke, A. (2010): Infrasound from Tungurahua Volcano 2006–2008: Strombolian to Plinian eruptive activity. Journal of Volcanology and Geothermal Research, 193 (1–2), 67–81.

Goerke, V. H., Young, J. M., and Cook, R. K. (1965): Infrasonic observations of the 1963 volcanic explosion on the island of Bali. J Geophys Res., 70, 6017–6022.

Heki, K. and Ping, J. S. (2005): Directivity and apparent velocity of the coseismic ionospheric disturbances observed with a dense GPS array. Earth Planet. Sci. Lett., 236, 845-855.

Kakinami, Y., Kamogawa, M., Tanioka, Y., Watanabe, S., Gusman, A. R., Liu, J. Y., Watanabe, Y., and Mogi, T. (2012): Tsunamigenic ionospheric hole. Geophys. Res. Lett., 39, L00G27, doi:10.1029/2011GL050159.

Le Pichon, A., Blanc, E., Drob, D., Lambotte, S., Dessa, J. X., Lardy, M., Bani, P., and Vergniolle, S., (2005): Infrasound monitoring of volcanoes to probe high-altitude winds. J Geophys Res., 110, D13106. doi:10.1029/2004JD005587.

Le Pichon, A., Herry, P., Mialle, P., Vergoz, J., Brachet, N., Garcés, M., Drob, D., and Ceranna, L. (2005): Infrasound associated with 2004–2005 large Sumatra earthquakes and tsunami. Geophys Res Lett., 32, L19802. doi:10.1029/2005GL023893.

Liszka, L., and Garcés, M. A. (2002): Infrasonic observations of the Hekla eruption of February 26, 2000, J. Low Freq. Noise, Vibration, and Active Control, 21, 1–8.

Liszka, L., and Hobara, Y. (2006): Sprite-attributed infrasonic chirps – their detections, occurrence and properties between 1994 and 2004. J Atmos Solar-Terrestrial Phys., 68, 1179–1188.

Zumberge, M. A., Berger, J., Hedlin, M. H., Husmann, E,. Nooner, S., Hilt, R., Widmer-Schnidrig, R. (2003): An optical fiber infrasound sensor: a new lower limit on atmospheric pressure noise between 1 and 10 Hz. J Acoust Soc Am., 113, 2474–2479.